HHS Public Access

Author manuscript

J Proteome Res. Author manuscript; available in PMC 2019 January 16.

Published in final edited form as:

J Proteome Res. 2015 April 03; 14(4): 1937–1946. doi:10.1021/pr5013152.

Modulation of Colon Cancer by Nutmeg

Fei Li[†,‡,⊥], **Xiu-Wei Yang**[*,§], **Kristopher W. Krausz**[†], **Robert G. Nichols**[‖], **Wei Xu**[§], **Andrew D. Patterson**[‖], and **Frank J. Gonzalez**[*,†]

[†] Laboratory of Metabolism, Center for Cancer Research, National Cancer Institute, National Institutes of Health, Bethesda, Maryland 20892, United States

[‡] Research Center for Differentiation and Development of Basic Theory of Traditional Chinese Medicine, Jiangxi University of Traditional Chinese Medicine, Nanchang 330004, China

[§] State Key Laboratory of Natural and Biomimetic Drugs, Department of Natural Medicines, School of Pharmaceutical Sciences, Peking University Health Science Center, Peking University, Beijing 100191, China

[‖] Center for Molecular Toxicology and Carcinogenesis, Department of Veterinary and Biomedical Sciences, The Pennsylvania State University, University Park, Pennsylvania 16802, United States

Abstract

Colon cancer is the most common cancer and the third leading cause of cancer mortality in humans. Using mass spectrometry-based metabolomics, the current study revealed the accumulation of four uremic toxins (cresol sulfate, cresol glucuronide, indoxyl sulfate, and phenyl sulfate) in the serum of mice harboring adenomatous polyposis coli (APC) gene mutation-induced colon cancer. These uremic toxins, likely generated from the gut microbiota, were associated with an increase in the expression of the proinflammatory cytokine IL-6 and a disorder of lipid metabolism. Nutmeg, which exhibits antimicrobial activity, attenuated the levels of uremic toxins and decreased intestinal tumorigenesis in $Apc^{min/+}$ mice. Nutmeg-treated $Apc^{min/+}$ mice had decreased IL-6 levels and normalized dysregulated lipid metabolism, suggesting that uremic toxins are responsible, in part, for the metabolic disorders that occur during tumorigenesis. These studies demonstrate a potential biochemical link among gut microbial metabolism, inflammation, and metabolic disorders and suggest that modulation of gut microbiota and lipid metabolism using dietary intervention or drugs may be effective in colon cancer chemoprevention strategies.

Graphical Abstract

[*]**Corresponding Authors:** (X.W.Y.) xwyang@bjmu.edu.cn; Fax: +86 10 82802724; Tel: +86-10-82805106., (F.J.G.) gonzalef@mail.nih.gov; Fax: 301-496-8419; Tel: 301-496-9067.

[⊥]**Present Address:** (F.L.) Office of Research, Center for Veterinary Medicine, U.S. Food and Drug Administration, 8401 Muirkirk Road, Laurel, Maryland 20708, United States.

The authors declare no competing financial interest.

Supporting Information

Table S1: qPCR primer sequences. Figure S1: Chemical composition of supercritical nutmeg extract. Figure S2: MS/MS fragmentation patterns of azelaic acid and cresol metabolites. Figure S3: Bile acid metabolism in $Apc^{min/+}$ mice. Figure S4: Increased bile acid levels in $Apc^{min/+}$ mice modulated by nutmeg treatment. Figure S5: Improvement of BUN in $Apc^{min/+}$ mice by nutmeg. Figure S6: The change of serum parameters following 4 month treatment with nutmeg extracts. Figure S7: Urinary excretion of uremic toxins in $Apc^{min/+}$ mice. This material is available free of charge via the Internet at http://pubs.acs.org.

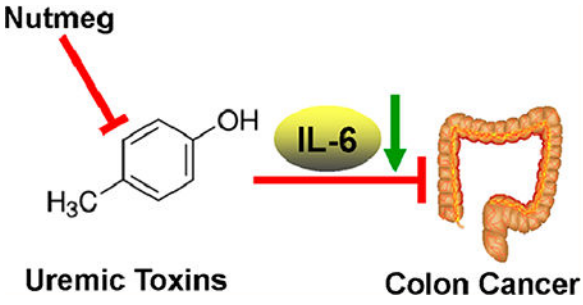

Keywords

Colon cancer; nutmeg; uremic toxin; inflammation; metabolomics; mass spectrometry

INTRODUCTION

Colon cancer is one of the most commonly diagnosed cancers and the third leading cause of cancer mortality in humans. It is widely accepted that the development of colon cancer is attributed to specific gene mutations and other nongenetic factors, notably, dietary components and the microbiota, which may influence spontaneous colon cancer.[1] Mutated genes that control cell division, apoptosis, and DNA repair have been identified in colon cancer, such as the adenomatous polyposis coli (APC) gene.[2] However, there is a limited understanding of how gut factors interact with genetic factors during colon carcinogenesis. Recently, using high-throughput metabolomics, a number of biomarkers for colon cancer were identified that might provide insight into the mechanism of colon cancer progression.[3,4] To date, approximately 300 metabolites were found to be up- or downregulated in the urine, serum, or colon tissue during colon cancer,[5] and most of these metabolites are involved in several major metabolic pathways, including glycolysis, the tricarboxylic acid cycle, and lipid, nucleotide, and amino acid metabolism. Many of these metabolic pathways are associated with the supply and demand of energy, resulting from the disruption of energy homeostasis during colon tumorigenesis. It was recently found that metabolites generated by the gut microbiota could be affected in colon cancer, including phenol, cresol sulfate, indoxyl sulfate, and hippurate.[6,7] Indeed, several studies revealed that the levels of the gut microbiota, including the phyla Proteobacteria, Bacteroidetes, and Firmicutes, were changed in the guts of colon cancer patients[8]

Microbes reside in the gut of healthy individuals, and it is known that changes in microbiota composition can affect different metabolic pathways, such as the metabolism of fatty acids and bile acids.[9,10] A number of studies revealed that the balance of gut microbiota is disrupted under pathological conditions, especially those associated with gastrointestinal diseases.[11–13] Among the complex microbiota in the intestine, the Gram-negative Proteobacteria with a lipopolysaccharide- containing outer membrane comprise the largest and most diverse phylum of bacteria, which show widespread pathogenic properties in the gastrointestinal tract.[14] Several bacteria in the Proteobacteria phylum such as *Helicobacter*, *Escherichia*, and *Campylobacter* are closely associated with stomach cancer, colon cancer, and inflammatory bowel diseases, including Crohn's disease and ulcerative colitis.[13,15,16]

Some studies have demonstrated the role of antibiotics as therapeutic agents in irritable bowel and inflammatory bowel diseases.[17,18]

Nutmeg, the seed of the fruit of *Myristica fragrans*, shows therapeutic efficacy in gastrointestinal disorders and is a widely used agent for the treatment of stomach ailments in China. Nutmeg is known to exhibit antimicrobial activity against the phylum Proteobacteria, especially *Helicobacter pylori* and *Escherichia coli*.[19,20] A recent study indicated that nutmeg can protect against dextran sulfate sodium-induced colitis in mice.[21] These observations provided a hint that nutmeg might prevent colon cancer via the modulation of inflammation and gut microbiota.

In the current study, mass spectrometry-based metabolomics was adopted to investigate the metabolic shifts in APC gene mutation-induced colon cancer, revealing changes in gut microbial metabolism and lipid metabolism in colon cancer. Furthermore, the antimicrobial and antioxidant potential of nutmeg can decrease the accumulation of uremic toxins, attenuate inflammation, and improve lipid metabolism in mice with colon cancer. This study demonstrates that nutmeg decreases colon cancer via modulating gut microbial metabolism and improving lipid metabolism.

MATERIALS AND METHODS

Chemicals and Reagents

Azelaic acid, undecanedioic acid, sebacic acid, citric acid, palmitic acid, palmitoleic acid, oleic acid, linoleic acid, phenyl sulfate, taurocholic acid (TCA), and taurodeoxycholic acid (TDCA) were purchased from Sigma-Aldrich (St. Louis, MO). 1-Palmitoyl-2-hydroxy-*sn*-glycero-3-phospho-ethanolamine (LPE 16:0), 1-stearoyl-2-hydroxy-*sn*-glycero-3-phosphoethanolamine (LPE 18:0), 1-oleoyl-2-hydroxy-*sn*-glycero-3-phosphoethanolamine (LPE 18:1), and 1-stearoyl-2-hydroxy-*sn*-glycero-3-phosphocholine (LPC 18:0) were obtained from Avanti Polar Lipids, Inc. (Alabaster, AL). Cresol sulfate and cresol glucuronide were synthesized as described previously.[22] All solvents and organic reagents were of the highest grade available.

Preparation of Nutmeg Extract

The dried ripe seeds of *M. fragrans* (nutmeg) were purchased from Indonesia in 2011 and characterized at the School of Pharmaceutical Sciences, Peking University Health Science Center, Peking University. A voucher specimen (no. 6396121RDK) was deposited at the State Key Laboratory of Natural and Biomimetic Drugs (Peking University). The carbon dioxide (CO_2) extract of nutmeg was obtained using CO_2 supercritical extraction as described previously.[23] The extraction and separation pressures were 20.0 and 8.0 MPa, respectively. The temperature of extraction and separation was 50.0 °C. The supercritical extracts of nutmeg consist of lignan, volatile oil, and fixed oil. Dehydrodiisoeugenol, myrislignan, and other major dihydrobenzofuran and 8-O-4′ type lignans can be detected in the methanol extracts of nutmeg (10 mg/ mL) (Supporting Information Figure 1).

Animal Studies and Treatments

Four week old male *Apc*$^{min/+}$ and wild-type mice on a C57BL/ 6J genetic background were obtained from the Jackson Laboratory and maintained under a standard 12 h light/12 h dark cycle with water and a normal diet (NIH-31) provided ad libitum. All mice were put on a synthetic purified diet (AIN-93G, Bio-Serv, NJ) for 5 days before the experiment. Twenty *Apc*$^{min/+}$ mice and wild-type mice were treated with the nutmeg-supplemented diet (AIN-93G supplemented with 2.5% CO_2 nutmeg extract, corresponding to the clinical dose of nutmeg used in humans) or vehicle diet (AIN-93G) for 4 months. Each group included five mice. One vehicle-fed *Apc*$^{min/+}$ mouse was found dead during the experiment. After 4 months of treatment and 4 h fasting, serum samples were collected from mice via retro-orbital bleeding. Colon, small intestine, and liver samples were harvested after the mice were killed by CO_2 asphyxiation, and tissues flash frozen in liquid nitrogen. All samples were stored at −80 °C until analysis. Mouse studies were performed under a protocol approved by the National Cancer Institute Animal Care and Use Committee.

UPLC−ESI−QTOFMS Analysis and Data Processing

Metabolites in the serum were detected by ultraperformance liquid chromatography coupled with electrospray ionization quadrupole time-of-flight mass spectrometry (UPLC−ESI−QTOFMS) (Waters Corp.), and the ion mass signals were processed by MarkerLynx software (Waters Corp.). Protein from serum samples was removed by adding 10 μL of serum to 190 μL of 67% aqueous acetonitrile and centrifuging at 14 000 rpm for 20 min at 4 °C. Chlorpropamide was added to the sample as an internal standard. A 5 μL aliquot of supernatant was separated using a 2.1 × 50 mm Waters BEH C18 1.7 μm column and introduced via electrospray into an UPLC−ESI− QTOFMS. The elution gradient of the mobile phase and the ionization parameters were consistent with those from previous studies.[24,25] Data were collected in full-scan mode from 100 to 1000 mass-to-charge ration (*m*/*z*), in both positive and negative modes. After generating the peak intensity, *m*/*z*, and retention time from the mass signals of ions using MarkerLynx, the peak intensity of all detected MS signals was normalized by the peak intensity of the internal standard, chlorpropamide. The multivariate data matrix was exported into SIMCA-P+13.0 (Umetrics, Kinnelon, NJ) for principal component analysis (PCA) and orthogonal partial least-squares discriminant analysis (OPLS-DA). UV scaling was used for multivariate analysis.

Identification and Quantitation of Serum Metabolites

The initial identity of high-contribution-score metabolites was searched using metabolomics databases (Madison Metabolomics Consortium Database and METLIN) to identify potential candidates. Serum biomarkers were further determined by comparison of their fragmentation patterns and retention times with those of authentic compounds. MS/MS fragmentations were obtained from serum samples and authentic standards (5−20 μM in 50% acetonitrile) under MS/MS fragmentation conditions with the collision energy ramping from 15 to 35 V. Quantitation of serum metabolites was performed using a Xevo triple quadrupole tandem MS (Waters Corp.) by multiple reaction monitoring (MRM). Serum samples were diluted 1:20 in 67% aqueous acetonitrile for all metabolites. A 5 μL sample of diluted serum and standards ranging from 0 to 25 μM were chromatographed on an Acquity 1.7 μm C18

column. Standard curves with correlation coefficients > 0.99 were used to quantify the metabolites in serum samples. The following MRM transitions were monitored: azelaic acid (187 → 124; ESI^-), sebacic acid (201 → 139; ESI^-), undecanedioic acid (215 → 153; ESI^-), cresol sulfate (187 → 106; ESI^-), cresol glucuronide (283 → 112; ESI^-), indoxyl sulfate (212 → 80; ESI^-), LPC 18:0 (524 → 104; ESI^+), LPE 18:1 (408 → 339 ESI^+), LPE 18:0 (482 → 341; ESI^+), LPE 16:0 (454 → 313; ESI^+), and chlorpropamide (277 → 110; ESI^+). Chlorpropamide (0.5 uM) was used as the internal standard.

Culture of Primary Hepatocytes and Caco-2 Cells

Primary hepatocytes were prepared from 6 week old C57BL/ 6N mice using the perfusion method.[9] Hepatocytes were isolated and purified by collagenase 1 perfusion (Invitrogen, Carlsbad, CA) and 45% Percoll density gradient centrifugation. Caco-2 cells (ATCC HTB-37) were seeded on a 24-well plate, and viability of the cells was measured using trypan blue dye exclusion; plates with viability higher than 85% were used for the experiment. After starvation for 4 h, hepatocytes and Caco-2 cells were exposed to 5 ng/mL IL-6 for 12 h and then collected and lysed for gene expression analysis using quantitative real-time PCR (qPCR).

Gene Expression Analysis

qPCR was used to quantify the levels of gene expression in the tissue. RNA was extracted using TRIzol reagent (Invitrogen, Carlsbad, CA) from cultured cells as well as frozen colon and liver tissues. Complementary DNA was generated from total RNA (1.0 mg) using Superscript II reverse transcriptase (Invitrogen, Carlsbad, CA). qPCR was carried out using SYBR green PCR mastermix (Applied Biosystems, Foster City, CA). Messenger RNA levels were normalized to those of β-actin mRNA. qPCR primer sequences are list in Supporting Information Table 1.

Serum Chemistry

Albumin, total protein, blood urea nitrogen (BUN), amylase, serum alkaline phosphatase (ALP), and other physiological serum parameters were measured using the VetScan VS2 comprehensive diagnostic profile (Abaxis, Inc., Union City, CA).

Data Analysis

Statistical analysis was performed using GraphPad Prism software (San Diego, CA). Two-tailed Student's *t* test and one-way ANOVA with Tukey's test and Dunnett's test were used to determine the differences in metabolites, gene expression, and bacteria between wild-type and $Apc^{min/+}$ mice and between vehicle- and nutmeg-treated $Apc^{min/+}$ mice. Experimental values are presented as the mean ± SEM; *P* values less than 0.05 are considered to be significant.

RESULTS

Global Profiling of Colon Cancer Using Metabolomics

Mutation of the APC gene leads to the early development of colon cancer, which can progress to invasive carcinoma.[26] The *Apc*$^{min/+}$ mouse, which carries a mutation in the *Apc* gene, develops colon cancer within 6 months of age.[27] In this study, the *Apc*$^{min/+}$ mouse model was used to determine the metabolic signatures for colon cancer. Colon tumors were observed in 5 month old *Apc*$^{min/+}$ mice, with some tumors reaching 2 mm (Figure 1A). Body mass was significantly decreased by 25% ($P < 0.05$) and 33% ($P < 0.01$) in 3 and 4 month old *Apc*$^{min/+}$ mice compared to that of the same age wild-type mice, respectively (Figure 1B). To determine the metabolic changes correlated with colon tumors, UPLC−ESI −QTOFMS-based metabolomics was used to screen the metabolites in serum from 5 month old *Apc*$^{min/+}$ mice by comparison with those in wild-type mice. The samples were analyzed by UPLC−ESI−QTOFMS in electrospray ionization positive (ESI^+) and negative (ESI^-) modes. After processing by MarkerLynx software and normalization to the internal standard, chlorpropamide, the data were subjected to multivariate data analysis. The quality control (QC) samples, including blanks, samples, and a cocktail of standards, showed good separation and reproducibility in the PCA model.[24] These QC data suggested that UPLC −ESI− QTOFMS was accurate, precise, and reproducible during the analysis. To directly identify potential candidate ions contributing to the separation of two groups, OPLS-DA models were constructed (Figure 1C). The differences between *Apc*$^{min/+}$ mice and wild-type mice were best described by OPLSDA, having an R^2 value of 1.0 and a Q^2 value of 0.91. In the *S*-plot of the OPLS-DA model, the levels of five ions (*m*/*z* 187.0065 at 1.54 min, *m*/*z* 212.0021 at 1.05 min, *m*/*z* 191.0188 at 0.31 min, *m*/*z* 172.9917 at 0.90 min, and *m*/*z* 514.2836 at 2.85 min) were significantly elevated in the serum of *Apc*$^{min/+}$ mice, whereas eight ions (*m*/*z* 187.0966 at 2.03 min, *m*/*z* 215.1275 at 2.68 min, *m*/*z* 201.1119 at 2.37 min, *m*/*z* 279.2324 at 5.86 min, *m*/*z* 281.2484 at 6.35 min, *m*/*z* 255.2321 at 6.22 min, *m*/*z* 568.3621 at 5.33 min, and *m*/*z* 480.3093 at 5.30 min) were markedly reduced (Figure 1D). The VIP values of these ions are provided in Table 1. All of these VIP values were higher than 1.0. These ions were initially subjected to database searches and tandem MS for identification. Identities were confirmed by tandem MS and retention time comparisons to authentic standards; several examples can be seen in Supporting Information Figure 2A–H for dicarboxylic acids, cresol, and sulfates. The enriched five metabolites were identified as cresol sulfate, indoxyl sulfate, citrate, phenyl sulfate, and TCA (Table 1). In contrast to the enriched metabolites, the eight attenuated ions are lipid metabolites: azelaic acid, sebacic acid, undecanedioic acid, linoleic acid, oleic acid, palmitic acid, LPC 18:0, and LPE 18:0 (Table 1). The most significantly enriched and attenuated metabolites were cresol sulfate (ion 9, VIP = 5.41) and azelaic acid (ion 1, VIP = 4.73) in the *S*-plot.

Colon Cancer Affected Gut Microbial Metabolism

Among the list of altered metabolites in the serum of *Apc*$^{min/+}$ mice with colon tumors (Table 1), the top elevated metabolites were cresol sulfate, indoxyl sulfate, and phenyl sulfate. The most significantly enriched metabolite in the *S*-plot, cresol sulfate, was increased 15-fold in *Apc*$^{min/+}$ mice compared to that in wild-type mice ($P < 0.01$), whereas cresol glucuronide had an average concentration of 70 μM in *Apc*$^{min/+}$ mice compared with

3.0 μM in wild-type mice (Figure 2A). Indoxyl sulfate's concentration increased from 0.9 μM in wild-type mice to 26 μM in *Apc*$^{min/+}$ mice ($P < 0.01$) (Figure 2A). Phenyl sulfate was elevated 10-fold in *Apc*$^{min/+}$ mice compared to that in wild-type mice ($P < 0.05$) (Figure 2B). It was demonstrated that cresol sulfate, cresol glucuronide, indoxyl sulfate, and phenyl sulfate are uremic toxins that are generated by gut bacteria,[28] suggesting that colon cancer affects metabolism carried out by the gut microbiota. Consistently, *Apc*$^{min/+}$ mice also showed higher bile acid levels in serum compared to that in wild-type mice in the *S*-plot (Figure 1D). The metabolism of bile acids and their levels are directly affected by the microbiota composition in the gut.[9,29] Triple quadrupole tandem MS quantitation indicated that the levels of TCA and TDCA in the serum were increased 12-fold ($P < 0.05$) and 5.8-fold ($P < 0.05$) in *Apc*$^{min/+}$ mice (Figure 2C), respectively. Furthermore, the expression of mRNAs encoding enzymes involved in the biosynthesis and transport of bile acids was significantly decreased in the livers of *Apc*$^{min/+}$ mice, including cytochrome P450 7A1 (*Cyp7a1*), Na^+-taurocholate cotransporting polypeptide (*Ntcp*), and bile salt export pump (*Bsep*) (Supporting Information Figure 3). These results suggest that colon cancer affects metabolism regulated by the gut microbiome, leading to the accumulation of uremic toxins and bile acids.

IL-6 Is a Regulator of Lipid Metabolism in Colon Cancer

Previous studies reported that uremic toxins can affect the function of a variety of cell types within the vascular system,[30] and some uremic toxins, such as cresol sulfate and cresol glucuronide, are associated with survival rates of hemodialysis patients.[31] In addition to the increased uremic toxins, OPLSDA modeling indicated that different lipid metabolites were lower in abundance in *Apc*$^{min/+}$ mice serum compared to that in wild-type mice, including free medium-chain dicarboxylic acids and long-chain fatty acids, along with phospholipids (Figure 1D). The levels of three dicarboxylic acids, azelaic acid, sebacic acid, and undecanedioic acid, were decreased from 35, 2.7, and 0.8 μM in wild-type mice to 10 μM ($P < 0.01$), 1.3 μM ($P < 0.01$), and 0.2 μM ($P < 0.01$) in *Apc*$^{min/+}$ mice ($P < 0.01$), respectively (Figure 3A). Linoleic acid, oleic acid, and palmitic acid were decreased 76% ($P < 0.01$), 74% ($P < 0.05$), and 36% ($P < 0.05$) in *Apc*$^{min/+}$ mice compared to that in wild-type mice (Figure 3B). LPC 18:0 and LPE 18:0, two phospholipids involved in cell signaling in the membrane, had average concentrations of 33 and 1.3 μM in *Apc*$^{min/+}$ mice compared with 70.7 μM ($P < 0.05$) and 2.0 μM ($P < 0.05$) in wild-type mice (Figure 3C). Target quantification revealed that the levels of LPE 16:0, LPE 18:1, and palmitoleic acid were downregulated 53% ($P < 0.05$), 47% ($P < 0.05$), and 85% ($P < 0.05$) in *Apc*$^{min/+}$ mice compared to that in wild-type mice (Figure 3B,C). The metabolomics results were further verified by direct fatty acid analysis, which revealed that total free fatty acids were reduced in *Apc*$^{min/+}$ mouse serum (Figure 3D). However, palmitoylcarnitine and oleoylcarnitine, which are biomarkers for the inhibition of fatty acid β-oxidation, were increased 1.7-fold ($P < 0.05$) and 1.6-fold ($P < 0.05$), respectively, in the *Apc*$^{min/+}$ mice compared to that in wild-type mice (Figure 3E), in agreement with the increased triglyceride concentrations in *Apc*$^{min/+}$ mouse serum (Figure 3D). These metabolite changes indicated a dysfunction of lipid metabolism associated with colon cancer in *Apc*$^{min/+}$ mice.

Previous studies revealed that cresol sulfate and cresol glucuronides are associated with the production of proinflammatory cytokines. Notably, increased cresol sulfate and indoxyl sulfate can upregulate interleukin 6 (IL-6) levels.[32] qPCR analysis indicated that the level of *Il-6* mRNA was increased 11-fold ($P < 0.01$) and 61-fold ($P < 0.01$) in the liver and colon tissues, respectively (Figure 4A). Serum albumin and total protein were decreased 80% ($P < 0.01$) and 49% ($P < 0.01$) in $Apc^{min/+}$ mice, confirming the generation of inflammation during colon tumorigenesis (Figure 4B). Serum chemistry analysis revealed that both serum blood urea nitrogen (BUN) and alanine aminotransferase (ALT) levels, which reflect the function of the kidney and liver, respectively, were increased more than 10-fold in $Apc^{min/+}$ mice compared to that in wild-type mice (Figure 4B–C). Serum amylase in $Apc^{min/+}$ mice was 2.4-fold ($P < 0.01$) of that in wild-type mice, which indicates possible intestinal obstruction by the colon tumor (Figure 4C). These observations suggested that the increase of uremic toxins caused inflammation in different organs and affected the function of colon, liver, and kidney. Gene expression analysis also indicated that mRNAs encoding fatty acid synthase (*Fasn*) and cytochrome P450 4A10 (*Cyp4a10*), involved in the synthesis and metabolism of fatty acids, were reduced by 69% ($P < 0.05$) and 55% ($P < 0.05$), respectively, in the colon of $Apc^{min/+}$ mice compared to that in wild-type mice, respectively (Figure 4D). Additionally, the expression of genes associated with synthesis and β-oxidation of fatty acids in the liver was also significantly inhibited in $Apc^{min/+}$ mice, including carnitine palmitoyltransferase II (*Cpt2*), acyl-CoA thioesterase I (*Acot1*), *Cyp4a10*, medium-chain acyl-CoA dehydrogenase (*Mcad*), and *Fasn* (Figure 4E). To examine whether the increased *IL-6* contributed to the dysregulated lipid metabolism, Caco-2 cells and primary hepatocytes were exposed to the active IL-6 protein. These results indicated that IL-6 exposure can downregulate *Cyp4a10* in both hepatocytes and Caco-2 cells (Figure 4F), suggesting that the increased IL-6 is responsible for the impaired fatty acid metabolism in the whole body. These results suggest that the accumulation of uremic toxins increased inflammation, as revealed by the elevation of IL-6, which is associated, in part, with the dysfunction of lipid metabolism in colon cancer.

Modulation of Gut Microbial and Lipid Metabolism by Nutmeg Decreased Colon Cancer

Nutmeg has been used traditionally for the treatment of gastrointestinal disorders.[19] In this study, nutmeg treatment decreased colon tumorigenesis in $Apc^{min/+}$ mice. The size and number of colon tumors were decreased 65% ($P < 0.05$) and 37% ($P < 0.05$) in nutmeg-treated $Apc^{min/+}$ mice compared to that in vehicle-treated $Apc^{min/+}$ mice, respectively (Figure 5A,B). PLS-DA models indicated significant difference among nutmeg-treated $Apc^{min/+}$ mice, vehicle-treated $Apc^{min/+}$ mice, nutmeg-treated wild-type mice, and vehicle-treated wild-type mice in the score scatter plot (Figure 5C) and revealed that more than 10 typical ions altered in the $Apc^{min/+}$ mice could be recovered by nutmeg in the loading scatter plot (Figure 5D). Specifically, three increased ions (m/z 187.0065 at 1.54 min, m/z 212.0021 at 1.05 min, and m/z 172.9917 at 0.90 min) during colon tumorigenesis were decreased in nutmeg-treated $Apc^{min/+}$ mice, whereas three ions (m/z 568.3621 at 5.33 min, m/z 480.3093 at 5.30 min, and m/z 187.0966 at 2.03 min) that decreased during tumorigenesis were increased by nutmeg treatment. Correspondingly, the levels of four uremic toxins, cresol sulfate, cresol glucuronide, indoxyl sulfate, and phenyl sulfate, were decreased 78% ($P < 0.01$), 77% ($P < 0.01$), 80% ($P < 0.01$), and 94% ($P < 0.05$) in the serum of nutmeg-treated

Apc$^{min/+}$ mice compared to that in vehicle-treated *Apc*$^{min/+}$ mice (Figure 6A,B). TDCA, a major bile acid that at high levels causes toxicity in the intestine, was also decreased 67% ($P < 0.01$) in nutmeg-treated *Apc*$^{min/+}$ mouse serum (Supporting Information Figure 4). The levels of *Il-6* mRNA were also downregulated 69% ($P < 0.01$) and 36% ($P < 0.05$) in the colon and liver of nutmeg-treated *Apc*$^{min/+}$ mice compared to that in vehicle-treated *Apc*$^{min/+}$ mice (Figure 6C). The level of serum BUN was attenuated 63% ($P < 0.05$) in *Apc*$^{min/+}$ mice by nutmeg treatment (Supporting Information Figure 5), whereas the level of ALT was decreased 93% ($P < 0.05$) by nutmeg (Figure 6D). The increased amylase levels in *Apc*$^{min/+}$ mice were downregulated 32% ($P < 0.05$) by nutmeg (Figure 6D). Serum chemistry analysis revealed no significant changes for the serum parameters ALT, total bilirubin, amylase, total protein, phosphorus, calcium, and potassium in nutmeg-treated WT mice compared to that in vehicle-treated WT mice (Figure 6D and Supporting Information Figure 6A–E), suggesting that a 4 month treatment at the current dose of nutmeg does not produce toxicity. These results suggested that nutmeg not only decreased colon tumorigenesis but also improved the impaired function of kidney, liver, and colon. In agreement with the lower IL-6 levels, nutmeg treatment can partly correct the dysregulated lipid metabolism in the colon cancer mice. Two phospholipids, LPC 18:0 and LPE 18:0, had average concentrations of 34 and 0.27 μM in nutmeg-treated *Apc*$^{min/+}$ mice compared with 55 μM ($P < 0.05$) and 0.46 μM ($P < 0.05$) in vehicle-treated *Apc*$^{min/+}$ mice ($P < 0.05$) (Figure 7A). The levels of two dicarboxylic acids, azelaic acid and sebacic acid, were increased 2- and 1.5-fold in nutmeg-treated *Apc*$^{min/+}$ mice compared to that in vehicle-treated *Apc*$^{min/+}$ mice ($P < 0.01$) (Figure 7B). Two elevated long-chain carnitines, palmitoylcarnitine and oleoylcarnitine, were decreased 51% ($P < 0.05$) and 50% ($P < 0.05$) in nutmeg-treated *Apc*$^{min/+}$ mice compared to that in vehicle-treated *Apc*$^{min/+}$ mice (Figure 7C). The expression of genes involved in the metabolism and synthesis of fatty acids was significantly elevated in the liver and colon in nutmeg-treated *Apc*$^{min/+}$ mice compared to that in vehicletreated *Apc*$^{min/+}$ mice, including *Cyp4a10* and *Cpt2* (Figure 7D). Colorimetric assays indicated that nutmeg treatment did not increase the levels of serum total fatty acids and triglyceride in WT mice (Supporting Information Figure 6F–G). These observations demonstrate that nutmeg extract prevents the mice from undergoing colon tumorigenesis via modulating gut microbial metabolism and improving dysregulated lipid metabolism.

DISCUSSION

The current study has demonstrated a significant metabolic shift in colon cancer. UPLC−ESI −QTOFMS was adopted to examine the metabolic signatures in *Apc*$^{min/+}$ mice by comparison with those in wild-type mice, revealing an accumulation of four uremic toxins, cresol sulfate, cresol glucuronide, indoxyl sulfate, and phenyl sulfate, in the serum. The accumulation of uremic toxins is correlated with increased IL-6 as well as lipid metabolism dysfunction in colon cancer. Furthermore, treatment with antimicrobial, antinflammatory, and antioxidant nutmeg resulted in a decrease in the number and size of tumors in *Apc*$^{min/+}$ mice, accompanied by decreased levels of uremic toxins and normalized lipid metabolism.

Using MS-based metabolomics analysis, we found that the levels of four uremic toxins, cresol sulfate, cresol glucuronide, indoxyl sulfate, and phenyl sulfate, were increased in the serum of *Apc*$^{min/+}$ mice. Under pathological conditions, such as deficient renal clearance,

uremic toxins cannot be normally excreted into urine, leading to elevated serum levels.[30] In *Apc*$^{min/+}$ mice, their levels were greatly increased in the serum, and their excretion in the urine was higher than that in wild-type mice (Supporting Information Figure 7), suggesting that kidney failure is not the cause of the accumulation of these conjugates. These uremic toxins are originally generated from the diet by the gut microbiota in vivo.[28,33–35] Previous studies reported that the levels of metabolites generated by gut microbiota were changed in the serum and urine of human colon cancer patients.[6,7] The phyla Proteobacteria, Bacteroidetes, and Firmicutes are prone to changes in the gut of colon cancer patients.[8] In particular, several bacteria in the phyla Proteobacteria are more prevalent in colon cancer patients, including *Eubacterium* spp., *Enterococcus faecalis*, and *Escherichia* spp.[8,36,37] These observations suggest that the alteration of gut microbiota in the context of colon cancer contributes to the generation of toxic metabolites.

Cresol sulfate, cresol glucuronide, indoxyl sulfate, and phenyl sulfate are small molecular uremic toxins that can bind protein and generate lipophilic uremic protein-binding toxins.[38] Among these protein-binding toxins, albumin-binding uremic toxins are widely generated and accumulate in the body, causing uremic toxicity.[31] Compared to wild-type mice, *Apc*$^{min/+}$ mice have lower levels of albumin and total protein in the serum, suggesting the generation of albumin-binding toxins. A recent study revealed that cresol sulfate and indoxyl sulfate enhance inflammation in proximal tubular cells, contributing to tubular damage and progression of renal failure.[32] In agreement with the current study, the levels of BUN were significantly elevated in *Apc*$^{min/+}$ mice compared to that in wild-type mice. Furthermore, nutmeg treatment decreased the accumulation of these four conjugates, and nutmeg-treated *Apc*$^{min/+}$ mice showed lower BUN levels, suggesting that these uremic toxins could be responsible, in part, for the renal failure associated with colon cancer. In agreement with a previous study, the increase in the four uremic toxins also demonstrated that changes in the gut microbiota during colon cancer impair the function of the gut−kidney axis.[39] In addition to renal failure, serum ALP levels were also increased in *Apc*$^{min/+}$ mice, suggesting that uremic toxins might cause whole body inflammation in these tumor-bearing mice. Indeed, studies have demonstrated that levels of cresol sulfate and indoxyl sulfate are correlated with increased inflammation and that they enhance the expression of pro-inflammatory cytokines, especially IL-6.[32] Indeed, expression of *Il-6* mRNA was increased in liver and colon of *Apc*$^{min/+}$ mice. Metabolomics revealed that colon cancer results in dysregulated lipid metabolism, which is probably a direct result of the increased expression of IL-6.[40] Furthermore, in vitro experiments indicated that IL-6 treatment can downregulate the level of *Cyp4a10* in both hepatocytes and Caco-2 cells, confirming that the increase in IL-6 may be responsible for the dysregulated lipid metabolism. In agreement with the current study, the level of hepatic *Cyp4a10* mRNA was downregulated in hepatic inflammation induced by *Citrobacter rodentium*, a strain in the phylum Proteobacteria.[41] These data provide evidence that modulation of gut microbial and lipid metabolism is an important therapeutic target for colon cancer.

Nutmeg is one of the most commonly used spices in the world and is prescribed for the treatment of gastrointestinal disorders in Asia. Nutmeg is known to exhibit strong antimicrobial activity against Gram-positive and -negative pathogenic bacteria, especially against *E. coli* and *H. pylori*.[19,20,42,43] In this study, treatment with the antimicrobial nutmeg

attenuated the accumulation of four uremic toxins produced by the gut microbiota in *Apc*$^{min/+}$ mice, leading to a decrease in tumorigenesis in *Apc*$^{min/+}$ mice. Microbial studies have demonstrated an expansion of the Proteobacteria phylum in patients with inflammatory bowel disease (IBD), which might drive proinflammatory changes and cause dysbiosis in the gut metabolism.[14] A recent study reported that nutmeg can protect against dextran sulfate sodium-induced IBD in mice and decrease the levels of proinflammatory cytokines in an IBD model.[21] These studies suggest the potential use of nutmeg for treatment of pathogenic bacteria associated with gastrointestinal diseases. While the exact mechanism of action by which nutmeg exerts its effects on pathogenic bacteria has not been completely elucidated, several antibacterial constituents isolated from nutmeg have been identified, such as macelignan[44] and trimyristin.[45] Tissue distribution studies also revealed that myrislignan and dehydrodiisoeugenol, two representative constituents in nutmeg, are higher in concentration in the intestine than in other tissues,[46,47] suggesting that high levels of nutmeg in the intestine contribute to inhibiting the growth of pathogenic bacteria. These results demonstrate that the gut microbiota and its metabolism regulated by nutmeg may be of therapeutic value against gastrointestinal diseases, including colon cancer and colitis.

Another important action of nutmeg is its antioxidant activity.[48] There are known antioxidants in nutmeg, including the terpene α/β-pinene and neolignan dehydrodiisoeugenol. Several new neolignans isolated from nutmeg exhibited potent anti-inflammatory activity in the RAW264.7 cell line stimulated with lipopolysaccharide.[23] Antioxidant supplements contribute to the reduction of different types of adenomas, especially for colon cancer.[49] It was demonstrated that colorectal cancer is linked to oxidative stress;[50,51] thus, antioxidants would be of value for the treatment and prevention of colorectal cancer. In one xenograft tumor model, metabolomics revealed that tumorigenesis can increase the concentration of asymmetric dimethylarginine in urine, indicating the production of oxidative stress in the body during tumorigenesis.[52] Oxidative stress can further activate the inflammatory cytokines that lead to the alteration of several metabolic pathways, including fatty acid oxidation, phospholipid metabolism, and the tricarboxylic acid cycle. A recent study reported that the levels of asymmetric dimethylarginine are significantly increased in the urine and tumor tissue of colon cancer patients and animal models, especially in *Apc*$^{min/+}$ mice.[53] Therefore, in addition to its antimicrobial activity, the antioxidant activity of nutmeg may also contribute to protection against colon cancer.

In summary, metabolomics revealed the accumulation of uremic toxins and the dysfunction of lipid metabolism in colon cancer. The elevation of IL-6 induced by uremic toxins is likely responsible for the dysregulated lipid metabolism. The decrease in colon cancer by antimicrobial nutmeg treatment supports the notion that the inflammation and metabolic disorder associated with colon cancer results from changes in gut microbial metabolism. The finding that nutmeg resulted in a decrease in colon cancer via regulating gut microbial metabolism and ameliorating metabolic disorders suggests that the modulation of the gut microbiota could act as a potential method for the treatment of colon cancer.

Supplementary Material

Refer to Web version on PubMed Central for supplementary material.

ACKNOWLEDGMENTS

The authors thank Drs. Naoki Tanaka and Changtao Jiang for assistance with the culture of primary hepatocytes and Caco-2 cells, respectively. This work was supported by a grant from the U.S.−China Program for Biomedical Collaborative Research and the National Cancer Institute Intramural Research Program to F.J.G., the National Natural Science Foundation of China (30973863 and 81161120429) to X.Y., and the National Natural Science Foundation of China (81360509) to F.L.

REFERENCES

(1). Watson AJ; Dubois RN Lipid metabolism and APC: implications for colorectal cancer prevention. Lancet 1997, 349, 444–5. [PubMed: 9040567]

(2). Kinzler KW; Vogelstein B Lessons from hereditary colorectal cancer. Cell 1996, 87, 159–70. [PubMed: 8861899]

(3). Chan EC; Koh PK; Mal M; Cheah PY; Eu KW; Backshall A; Cavill R; Nicholson JK; Keun HC Metabolic profiling of human colorectal cancer using high-resolution magic angle spinning nuclear magnetic resonance (HR-MAS NMR) spectroscopy and gas chromatography mass spectrometry (GC/MS). J. Proteome Res 2009, 8, 352–61. [PubMed: 19063642]

(4). Hirayama A; Kami K; Sugimoto M; Sugawara M; Toki N; Onozuka H; Kinoshita T; Saito N; Ochiai A; Tomita M; Esumi H; Soga T Quantitative metabolome profiling of colon and stomach cancer microenvironment by capillary electrophoresis time-of-flight mass spectrometry. Cancer Res. 2009, 69, 4918–25. [PubMed: 19458066]

(5). Williams MD; Reeves R; Resar LS; Hill HH, Jr. Metabolomics of colorectal cancer: past and current analytical platforms. Anal. Bioanal. Chem 2013, 405, 5013–30. [PubMed: 23494270]

(6). Cheng Y; Xie G; Chen T; Qiu Y; Zou X; Zheng M; Tan B; Feng B; Dong T; He P; Zhao L; Zhao A; Xu LX; Zhang Y; Jia W Distinct urinary metabolic profile of human colorectal cancer. J. Proteome Res 2012, 11, 1354–63. [PubMed: 22148915]

(7). Qiu Y; Cai G; Su M; Chen T; Zheng X; Xu Y; Ni Y; Zhao A; Xu LX; Cai S; Jia W Serum metabolite profiling of human colorectal cancer using GC-TOFMS and UPLC-QTOFMS. J. Proteome Res 2009, 8, 4844–50. [PubMed: 19678709]

(8). Wang T; Cai G; Qiu Y; Fei N; Zhang M; Pang X; Jia W; Cai S; Zhao L Structural segregation of gut microbiota between colorectal cancer patients and healthy volunteers. ISME J. 2012, 6, 320–9. [PubMed: 21850056]

(9). Li F; Jiang C; Krausz KW; Li Y; Albert I; Hao H; Fabre KM; Mitchell JB; Patterson AD; Gonzalez FJ Microbiome remodelling leads to inhibition of intestinal farnesoid X receptor signalling and decreased obesity. Nat. Commun 2013, 4, 2384. [PubMed: 24064762]

(10). Donohoe DR; Garge N; Zhang X; Sun W; O'Connell TM; Bunger MK; Bultman SJ The microbiome and butyrate regulate energy metabolism and autophagy in the mammalian colon. Cell Metab. 2011, 13, 517–26. [PubMed: 21531334]

(11). Hsiao EY; McBride SW; Hsien S; Sharon G; Hyde ER; McCue T; Codelli JA; Chow J; Reisman SE; Petrosino JF; Patterson PH; Mazmanian SK Microbiota modulate behavioral and physiological abnormalities associated with neurodevelopmental disorders. Cell 2013, 155, 1451–63. [PubMed: 24315484]

(12). Turnbaugh PJ; Gordon JI An invitation to the marriage of metagenomics and metabolomics. Cell 2008, 134, 708–13. [PubMed: 18775300]

(13). Newman A; Lambert JR *Campylobacter jejuni* causing flareup in inflammatory bowel disease. Lancet 1980, 2, 919.

(14). Mukhopadhya I; Hansen R; El-Omar EM; Hold GL IBDwhat role do Proteobacteria play? Nat. Rev. Gastroenterol. Hepatol 2012, 9, 219–30. [PubMed: 22349170]

(15). el-Omar E; Penman I; Cruikshank G; Dover S; Banerjee S; Williams C; McColl KE Low prevalence of *Helicobacter pylori* in inflammatory bowel disease: association with sulphasalazine. Gut 1994, 35, 1385–8. [PubMed: 7959192]

(16). Martin HM; Campbell BJ; Hart CA; Mpofu C; Nayar M; Singh R; Englyst H; Williams HF; Rhodes JM Enhanced *Escherichia coli* adherence and invasion in Crohn's disease and colon cancer. Gastroenterology 2004, 127, 80–93. [PubMed: 15236175]

(17). Hviid A; Svanstrom H; Frisch M Antibiotic use and inflammatory bowel diseases in childhood. Gut 2011, 60, 49–54. [PubMed: 20966024]

(18). Khan KJ; Ullman TA; Ford AC; Abreu MT; Abadir A; Marshall JK; Talley NJ; Moayyedi P Antibiotic therapy in inflammatory bowel disease: a systematic review and meta-analysis. Am. J. Gastroenterol 2011, 106, 661–73. [PubMed: 21407187]

(19). Mahady GB; Pendland SL; Stoia A; Hamill FA; Fabricant D; Dietz BM; Chadwick LR In vitro susceptibility of *Helicobacter pylori* to botanical extracts used traditionally for the treatment of gastrointestinal disorders. Phytother Res. 2005, 19, 988–91. [PubMed: 16317658]

(20). De M; Krishna De A; Banerjee AB Antimicrobial screening of some Indian spices. Phytother. Res 1999, 13, 616–8. [PubMed: 10548758]

(21). Kim H; Bu Y; Lee BJ; Bae J; Park S; Kim J; Lee K; Cha JM; Ryu B; Ko SJ; Han G; Min B; Park JW Myristica fragrans seed extract protects against dextran sulfate sodium-induced colitis in mice. J. Med. Food 2013, 16, 953–6. [PubMed: 24063406]

(22). Cho JY; Matsubara T; Kang DW; Ahn SH; Krausz KW; Idle JR; Luecke H; Gonzalez FJ Urinary metabolomics in Fxr-null mice reveals activated adaptive metabolic pathways upon bile acid challenge. J. Lipid Res 2010, 51, 1063–74. [PubMed: 19965603]

(23). Cao G; Xu W; Yang XW; Gonzalez FJ; Li F New neolignans from the seeds of *Myristica fragrans* that inhibit nitric oxide production. Food Chem. 2015, 173, 231–237. [PubMed: 25466017]

(24). Li F; Pang X; Krausz KW; Jiang C; Chen C; Cook JA; Krishna MC; Mitchell JB; Gonzalez FJ; Patterson AD Stable isotope- and mass spectrometry-based metabolomics as tools in drug metabolism: a study expanding tempol pharmacology. J. Proteome Res 2013, 12, 1369–76. [PubMed: 23301521]

(25). Li F; Jiang C; Larsen MC; Bushkofsky J; Krausz KW; Wang T; Jefcoate CR; Gonzalez FJ Lipidomics reveals a link between CYP1B1 and SCD1 in promoting obesity. J. Proteome Res 2014, 13, 2679–87. [PubMed: 24684199]

(26). Ceol CJ; Pellman D; Zon LI APC and colon cancer: two hits for one. Nat. Med 2007, 13, 1286–7. [PubMed: 17987022]

(27). Heyer J; Yang K; Lipkin M; Edelmann W; Kucherlapati R Mouse models for colorectal cancer. Oncogene 1999, 18, 5325–33. [PubMed: 10498885]

(28). Nicholson JK; Holmes E; Kinross J; Burcelin R; Gibson G; Jia W; Pettersson S Host−gut microbiota metabolic interactions. Science 2012, 336, 1262–7. [PubMed: 22674330]

(29). Sayin SI; Wahlstrom A; Felin J; Jantti S; Marschall HU; Bamberg K; Angelin B; Hyotylainen T; Oresic M; Backhed F Gut microbiota regulates bile acid metabolism by reducing the levels of tauro-beta-muricholic acid, a naturally occurring FXR antagonist. Cell Metab. 2013, 17, 225–35. [PubMed: 23395169]

(30). Vanholder R; Baurmeister U; Brunet P; Cohen G; Glorieux G; Jankowski J; European Uremic Toxin Work Group. A bench to bedside view of uremic toxins. J. Am. Soc. Nephrol 2008, 19, 863–70. [PubMed: 18287557]

(31). Meijers BK; De Loor H; Bammens B; Verbeke K; Vanrenterghem Y; Evenepoel P *p*-Cresyl sulfate and indoxyl sulfate in hemodialysis patients. Clin. J. Am. Soc. Nephrol 2009, 4, 1932–8. [PubMed: 19833905]

(32). Sun CY; Hsu HH; Wu MS p-Cresol sulfate and indoxyl sulfate induce similar cellular inflammatory gene expressions in cultured proximal renal tubular cells. Nephrol., Dial., Transplant 2013, 28, 70–8. [PubMed: 22610984]

(33). Li JV; Ashrafian H; Bueter M; Kinross J; Sands C; le Roux CW; Bloom SR; Darzi A; Athanasiou T; Marchesi JR; Nicholson JK; Holmes E Metabolic surgery profoundly influences gut microbial −host metabolic cross-talk. Gut 2011, 60, 1214–23. [PubMed: 21572120]

(34). Hida M; Aiba Y; Sawamura S; Suzuki N; Satoh T; Koga Y Inhibition of the accumulation of uremic toxins in the blood and their precursors in the feces after oral administration of lebenin, a lactic acid bacteria preparation, to uremic patients undergoing hemodialysis. Nephron 1996, 74, 349–55. [PubMed: 8893154]

(35). Achkar J; Xian M; Zhao H; Frost JW Biosynthesis of phloroglucinol. J. Am. Chem. Soc 2005, 127, 5332–3. [PubMed: 15826166]

(36). Moore WE; Moore LH Intestinal floras of populations that have a high risk of colon cancer. Appl. Environ. Microbiol 1995, 61, 3202–7. [PubMed: 7574628]

(37). Balamurugan R; Rajendiran E; George S; Samuel GV; Ramakrishna BS Real-time polymerase chain reaction quantification of specific butyrate-producing bacteria, Desulfovibrio and Enterococcus faecalis in the feces of patients with colorectal cancer. J. Gastroenterol. Hepatol 2008, 23, 1298–303. [PubMed: 18624900]

(38). Liabeuf S; Drueke TB; Massy ZA Protein-bound uremic toxins: new insight from clinical studies. Toxins 2011, 3, 911–9. [PubMed: 22069747]

(39). Meijers BK; Evenepoel P The gut−kidney axis: indoxyl sulfate, p-cresyl sulfate and CKD progression. Nephrol., Dial., Transplant 2011, 26, 759–61. [PubMed: 21343587]

(40). Katsume A; Saito H; Yamada Y; Yorozu K; Ueda O; Akamatsu K; Nishimoto N; Kishimoto T; Yoshizaki K; Ohsugi Y Anti-interleukin 6 (IL-6) receptor antibody suppresses Castleman's disease like symptoms emerged in IL-6 transgenic mice. Cytokine 2002, 20, 304–11. [PubMed: 12633573]

(41). Richardson TA; Sherman M; Antonovic L; Kardar SS; Strobel HW; Kalman D; Morgan ET Hepatic and renal cytochrome p450 gene regulation during citrobacter rodentium infection in wild-type and toll-like receptor 4 mutant mice. Drug Metab. Dispos 2006, 34, 354–60. [PubMed: 16339354]

(42). O'Mahony R; Al-Khtheeri H; Weerasekera D; Fernando N; Vaira D; Holton J; Basset C Bactericidal and anti-adhesive properties of culinary and medicinal plants against *Helicobacter pylori*. World J. Gastroenterol 2005, 11, 7499–507. [PubMed: 16437723]

(43). Takikawa A; Abe K; Yamamoto M; Ishimaru S; Yasui M; Okubo Y; Yokoigawa K Antimicrobial activity of nutmeg against *Escherichia coli* O157. J. Biosci. Bioeng 2002, 94, 315–20. [PubMed: 16233309]

(44). Chung JY; Choo JH; Lee MH; Hwang JK Anticariogenic activity of macelignan isolated from Myristica fragrans (nutmeg) against Streptococcus mutans. Phytomedicine 2006, 13, 261–6. [PubMed: 16492529]

(45). Narasimhan B; Dhake AS Antibacterial principles from Myristica fragrans seeds. J. Med. Food 2006, 9, 395−9. [PubMed: 17004905]

(46). Li F; Yang XW Determination of dehydrodiisoeugenol in rat tissues using HPLC method. Biomed. Chromatogr 2008, 22, 1206–12. [PubMed: 18651609]

(47). Wang Y; Liu J; Zhang Y; Li F; Yang XW Determination and distribution study of myrislignan in rat by RP-HPLC. Chromatographia 2012, 75, 541–9.

(48). Murcia MA; Egea I; Romojaro F; Parras P; Jimenez AM; Martinez-Tome M Antioxidant evaluation in dessert spices compared with common food additives. Influence of irradiation procedure. J. Agric. Food Chem 2004, 52, 1872–81. [PubMed: 15053523]

(49). Bonelli L; Puntoni M; Gatteschi B; Massa P; Missale G; Munizzi F; Turbino L; Villanacci V; De Censi A; Bruzzi P Antioxidant supplement and long-term reduction of recurrent adenomas of the large bowel. A double-blind randomized trial. J. Gastroenterol 2013, 48, 698–705. [PubMed: 23065023]

(50). Chang D; Wang F; Zhao YS; Pan HZ Evaluation of oxidative stress in colorectal cancer patients. Biomed. Environ. Sci 2008, 21, 286–9. [PubMed: 18837290]

(51). Perse M Oxidative stress in the pathogenesis of colorectal cancer: cause or consequence? Biomed. Res. Int 2013, 2013, 725710. [PubMed: 23762854]

(52). Li F; Patterson AD; Krausz KW; Jiang C; Bi H; Sowers AL; Cook JA; Mitchell JB; Gonzalez FJ Metabolomics reveals that tumor xenografts induce liver dysfunction. Mol. Cell. Proteomics 2013, 12, 2126–35. [PubMed: 23637421]

(53). Manna SK; Tanaka N; Krausz KW; Haznadar M; Xue X; Matsubara T; Bowman ED; Fearon ER; Harris CC; Shah YM; Gonzalez FJ Biomarkers of coordinate metabolic reprogramming in colorectal tumors in mice and humans. Gastroenterology 2014, 146, 1313–24. [PubMed: 24440673]

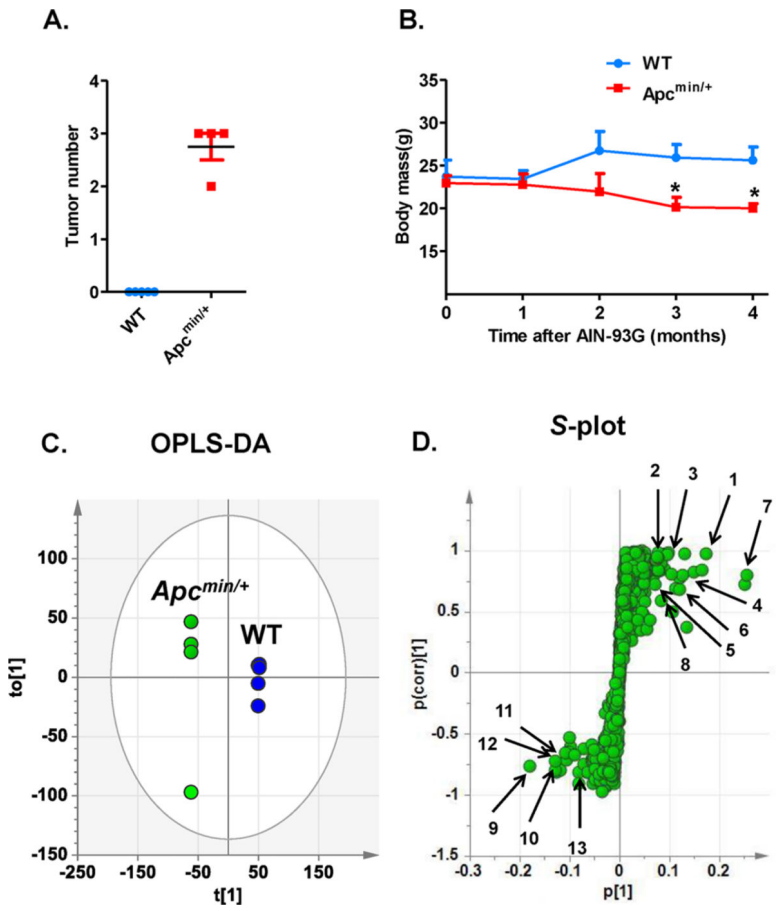

Figure 1.

Metabolomics analysis of serum metabolites in colon cancer. (A) Tumor number (tumor diameter > 1 mm) in the colon of *Apc*$^{min/+}$ mice after 4 months receiving AIN-93G feed. (B) Body weight of *Apc*$^{min/+}$ mice and wild-type (WT) mice from 0 to 4 months after receiving AIN-93G feed. (C) OPLS-DA model of serum sample from WT (n = 4, blue) and *Apc*$^{min/+}$ mice (n = 4, green). (D) Scatter plot of OPLS-DA model. The labeled ions are the metabolites contributing to the separation of *Apc*$^{min/+}$ mice from WT mice. Metabolite codes correspond to those in listed Table 1. The p_{corr}[1] P values represent the interclass differences, and p[1] P values represent the relative abundance of the ions. All data were obtained in negative mode (ESI$^-$) by UPLC−ESI−QTOFMS. Statistical analysis was performed using two-tailed Student's t test and ANOVA (n = 4 in each group). *, $P < 0.05$ compared to WT mice.

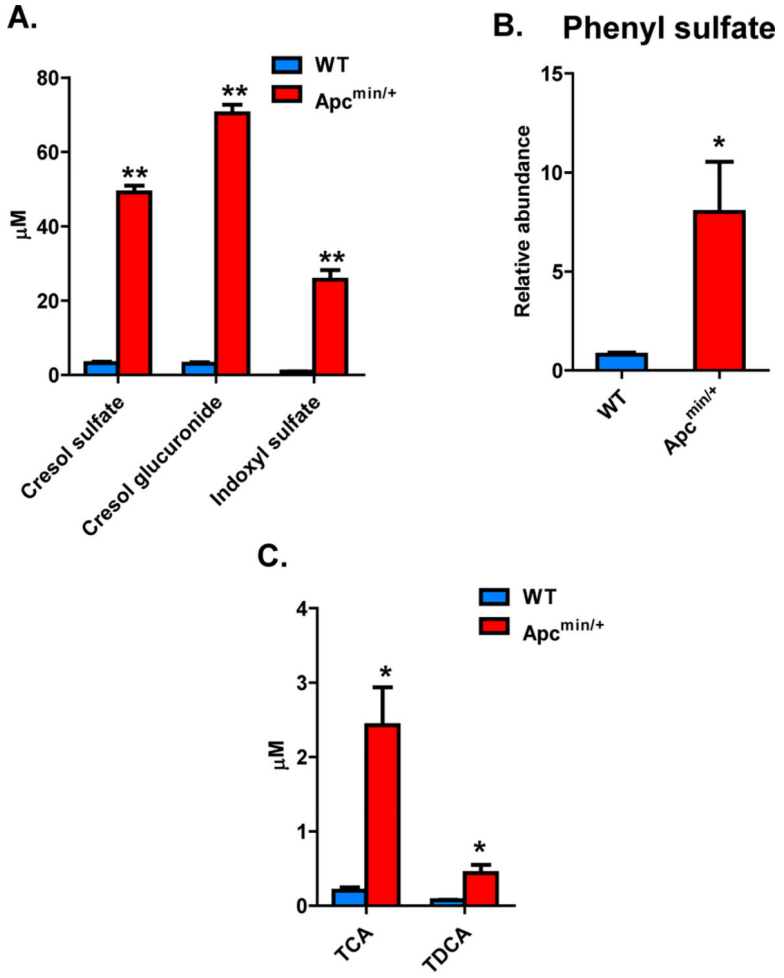

Figure 2.

Gut microbiota metabolism was affected by colon cancer. (A) Serum levels of cresol sulfate, cresol glucuronide, and indoxyl sulfate in 5 month old WT and *Apc*$^{min/+}$ mice. (B) Phenyl sulfate levels in 5 month old WT and *Apc*$^{min/+}$ mice. (C) Serum levels of TCA and TDCA in 5 month old WT and *Apc*$^{min/+}$ mice. Statistical analysis was performed using two-tailed Student's *t* test and ANOVA ($n = 4$ in each group). *, $P < 0.05$ and **, $P < 0.01$ compared to WT mice.

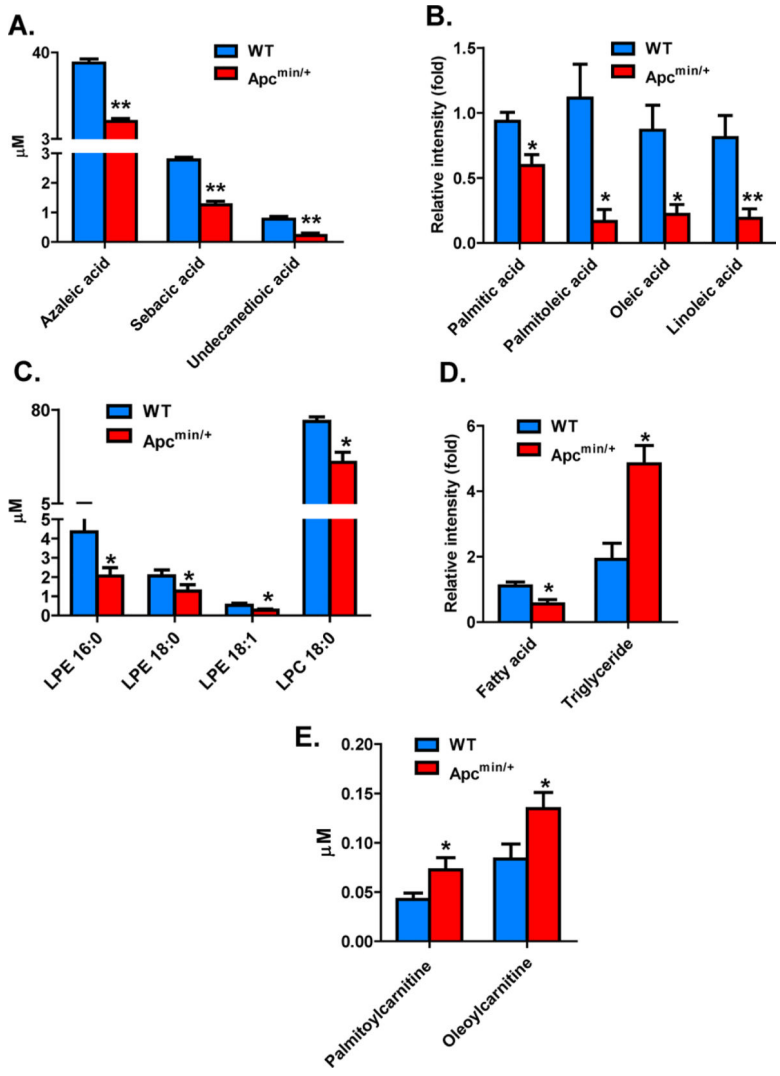

Figure 3.

Colon cancer induces dysfunction in lipid metabolism. (A) Serum levels of azelaic acid, sebacic acid, and undecanedioic acid in 5 month old WT and *Apc*$^{min/+}$ mice. (B) Levels of palmitic acid, palmitoleic acid, oleic acid, and linoleic acid in the serum of 5 month old WT and *Apc*$^{min/+}$ mice. (C) LPE 16:0, LPE 18:0, LPE 18:1, and LPC 18:0 levels in the serum of 5 month old WT and *Apc*$^{min/+}$ mice. (D) Total levels of free fatty acid and triglyceride in the serum of 5 month old WT and *Apc*$^{min/+}$ mice. (E) Serum levels of palmitoylcarnitine and oleoylcarnitine in 5 month old WT and *Apc*$^{min/+}$ mice. Statistical analysis was performed using two-tailed Student's *t* test and ANOVA ($n = 4$ in each group). *, $P < 0.05$ and **, $P < 0.01$ compared to WT mice.

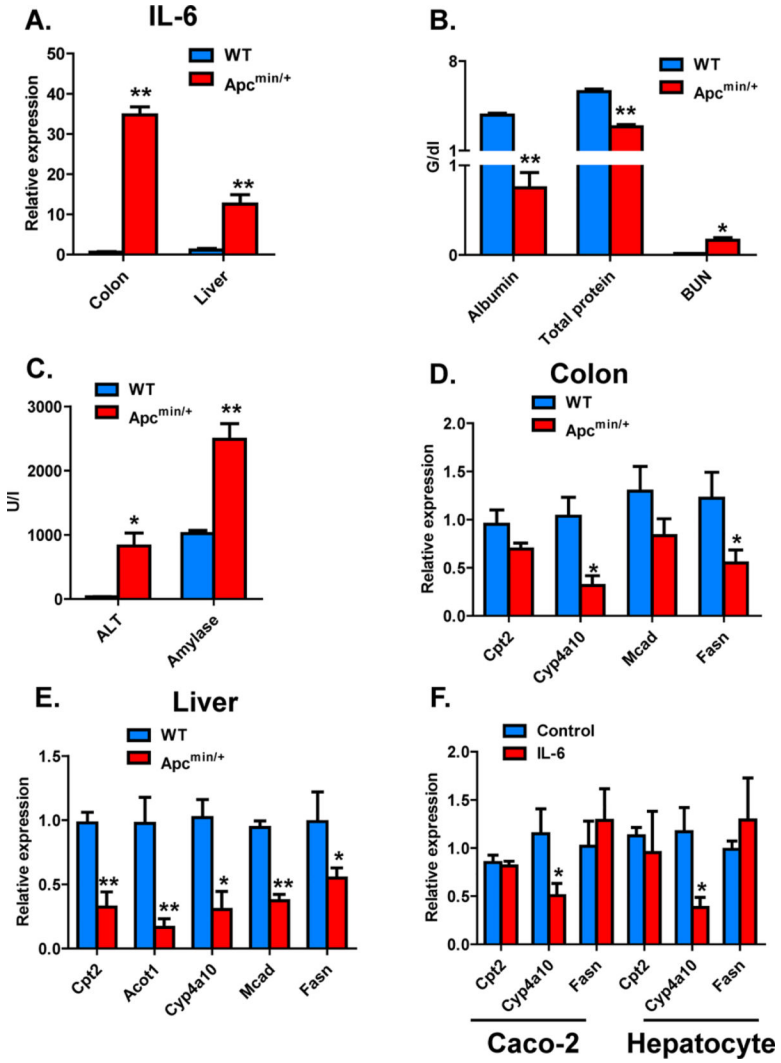

Figure 4.

IL-6 regulates lipid metabolism in colon cancer. (A) qPCR analysis of *IL-6* mRNA levels in the colon and liver of 5 month old WT and *Apc*$^{min/+}$ mice. (B) Levels of serum albumin, total protein, and blood urea nitrogen in 5 month old WT and *Apc*$^{min/+}$ mice. (C) Levels of serum ALT and amylase in 5 month old WT and *Apc*$^{min/+}$ mice. (D) qPCR analysis of the mRNAs encoding enzymes associated with fatty acid synthesis and *β*-oxidation in the colon of 5 month old WT and *Apc*$^{min/+}$ mice. (E) Hepatic mRNA levels of *Cpt2*, *Acot1*, *Cyp4a10*, *Mcad*, and *Fasn* in 5 month old WT and *Apc*$^{min/+}$ mice. (F) *Cpt2*, *Cyp4a10*, and *Fasn* mRNA expression of Caco-2 cells and hepatocytes after exposure to 5 ng/mL IL-6. The mRNA levels were normalized to those of *β-actin* mRNA. Statistical analysis was performed using two-tailed Student's *t* test and ANOVA ($n = 4$ in each group). *, $P < 0.05$ and **, $P < 0.01$ compared to WT mice.

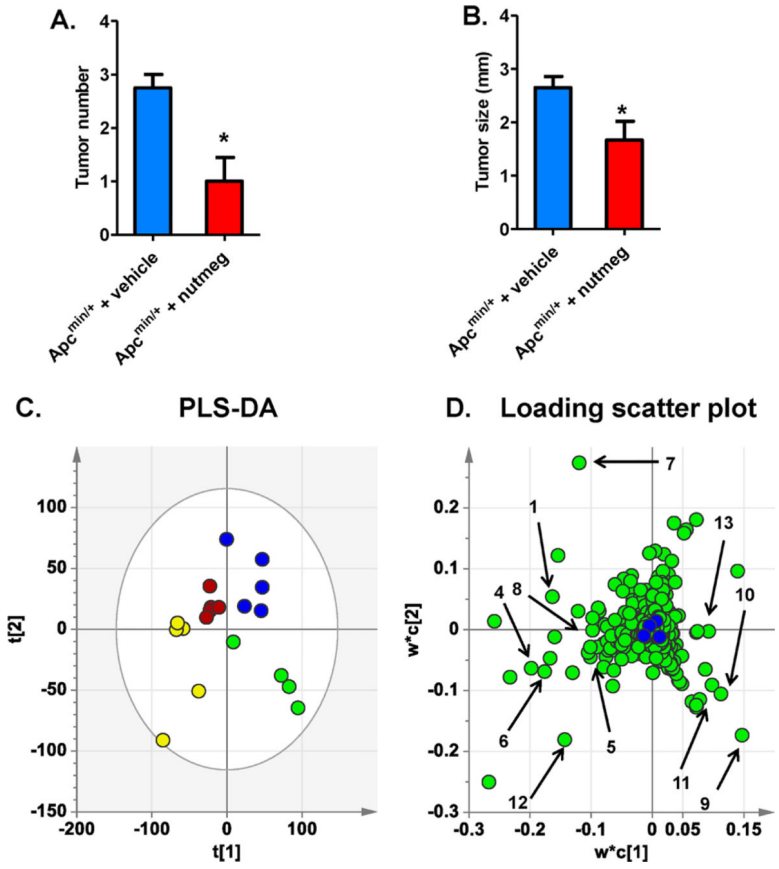

Figure 5.

Nutmeg inhibits colon tumorigenesis. (A) Tumor number (tumor diameter > 1 mm) in the colon of *Apc*$^{min/+}$ mice after nutmeg treatment for 4 months. (B) Size of colon tumors in *Apc*$^{min/+}$ mice after nutmeg treatment for 4 months. (C) PLS-DA model of serum samples from nutmeg-fed *Apc*$^{min/+}$ mice ($n = 5$, blue), vehicle-fed *Apc*$^{min/+}$ mice ($n = 4$, green), nutmeg-fed WT mice ($n = 5$, yellow), and vehicle-fed WT mice ($n = 5$, red). (D) Loading scatter plot of the PLS-DA model. Metabolite codes correspond to those in Table 1. All data were obtained in negative mode (ESI^-) by UPLC−ESI− QTOFMS. Statistical analysis was performed using two-tailed Student's *t* test and ANOVA ($n = 4/5$ in each group). *, $P < 0.05$ compared to vehicle-fed *Apc*$^{min/+}$ mice.

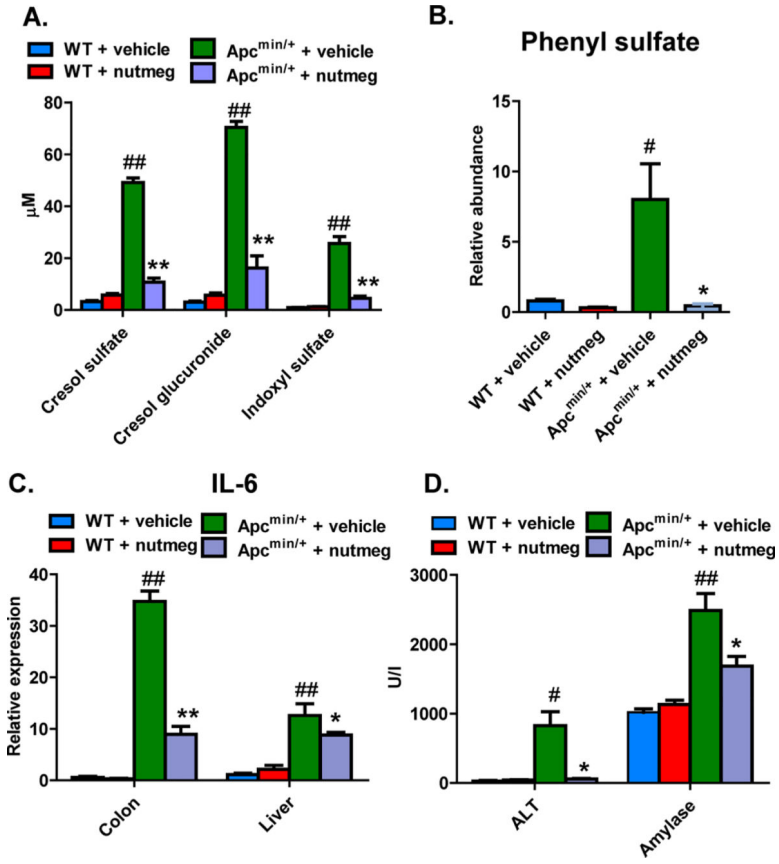

Figure 6.

Nutmeg attenuates the accumulation of uremic toxins and inflammation in colon cancer. (A, B) Serum levels of cresol sulfate, cresol glucuronide, phenyl sulfate, and indoxyl sulfate in nutmeg-fed *Apc*$^{min/+}$ and WT mice, and vehicle-fed *Apc*$^{min/+}$ and WT mice. (C) qPCR analysis of *IL-6* levels in the colon and liver of *Apc*$^{min/+}$ mice after nutmeg treatment for 4 months. (D) Levels of serum ALT and amylase in nutmeg-fed *Apc*$^{min/+}$ mice compared to that in the other groups. Statistical analysis was performed using two-tailed Student's *t* test and ANOVA ($n = 4/5$ in each group). *, $P < 0.05$ and **, $P < 0.01$ compared to vehicle-fed *Apc*$^{min/+}$ mice; #, $P < 0.05$ and ##, $P < 0.01$ compared to vehicle-fed WT mice.

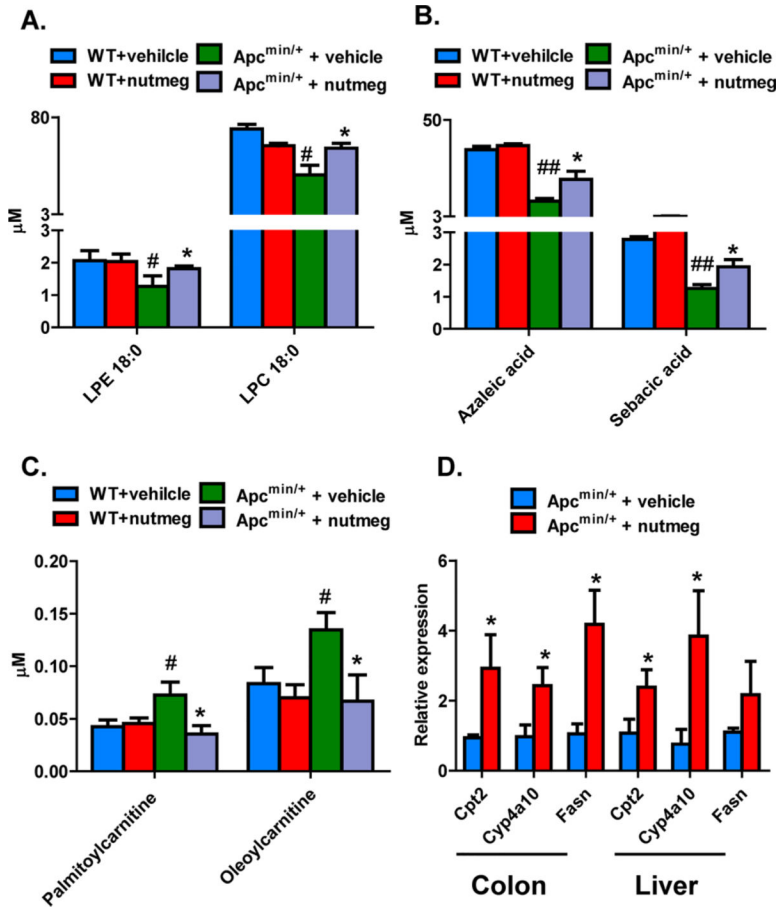

Figure 7.

Nutmeg leads to recovery of the impaired lipid metabolism in colon cancer. (A) Levels of LPE 18:0 and LPC 18:0 in the serum of *Apc*$^{min/+}$ mice after nutmeg treatment for 4 months. (B) Serum levels of azelaic acid and sebacic acid in nutmeg-fed *Apc*$^{min/+}$ and WT mice compared to that in vehicle-fed *Apc*$^{min/+}$ and WT mice. (C) Serum levels of palmitoylcarnitine and oleoylcarnitine in nutmeg-fed *Apc*$^{min/+}$ mice after nutmeg treatment for 4 months. (D) qPCR analysis of the genes associated with fatty acid synthesis and metabolism in nutmeg-fed *Apc*$^{min/+}$ mice compared to that in vehicle-fed *Apc*$^{min/+}$ mice. The mRNA levels were normalized to those of *β-actin* mRNA. Statistical analysis was performed using two-tailed Student's t test and ANOVA (n = 4/5 in each group). *, $P < 0.05$ and **, $P < 0.01$ compared to vehicle-fed *Apc*$^{min/+}$ mice; #, $P < 0.05$ and ##, $P < 0.01$ compared to vehicle-fed WT mice.

Table 1.

Summary of Ions Altered in *Apc*$^{min/+}$ Mice Compared to Those in WT Mice

ion	t_R (min)	mass (*m*/*z*)	empirical formula	mass error (ppm)	VIP value	identity
Downregulation						
1	2.03	187.0966	$C_9H_{15}O_4$ [H−]	−2.1	4.73	azelaic acid
2	2.37	201.1119	$C_{10}H_{18}O_4$ [H−]	−3.5	1.22	sebacic acid
3	2.68	215.1275	$C_{11}H_{20}O_4$ [H−]	−3.7	1.43	undecanedioic acid
4	5.86	279.2324	$C_{18}H_{32}O_2$ [H−]	0	4.24	linoleic acid
5	6.22	255.2321	$C_{18}H_{34}O_2$ [H−]	−1.1	2.01	oleic acid
6	6.35	281.2484	$C_{16}H_{32}O_2$ [H−]	1.4	3.58	palmitic acid
7	5.33	568.3621	$C_{27}H_{56}NO_9P$ [HCO_2H−]	1.2	7.51	LPC 18:0
8	5.30	480.3093	$C_{23}H_{48}NO_7P$ [H−]	0.6	1.47	LPE 18:0
Upregulation						
9	1.54	187.0065	$C_7H_8O_4S$ [H−]	0	5.41	cresol sulfate
10	1.05	212.0021	$C_8H_7NO_4S$ [H−]	1.8	3.82	indoxyl sulfate
11	0.91	172.9917	$C_6H_6O_4S$ [H−]	5.2	3.33	phenyl sulfate
12	2.85	514.2836	$C_{26}H_{45}NO_7S$ [H−]	−0.4	3.46	taurocholic acid
13	0.31	191.0188	$C_6H_8O_7$ [H−]	−1.6	2.32	citrate